

# Chromophore Structure in the Photocycle of the Cyanobacterial Phytochrome Cph1

Jasper J. van Thor,\* Mukram Mackeen,<sup>†</sup> Ilya Kuprov,<sup>‡</sup> Raymond A. Dwek,<sup>†</sup> and Mark R. Wormald<sup>†</sup>

\*Laboratory of Molecular Biophysics, <sup>†</sup>Oxford Glycobiology Institute, Department of Biochemistry, and <sup>‡</sup>Department of Chemistry, Physical and Theoretical Chemistry Laboratory, University of Oxford, Oxford OX1 3QZ, United Kingdom

- [AQ1]** **ABSTRACT** The chromophore conformations of the red and far red light induced product states “Pfr” and “Pr” of the N-terminal photoreceptor domain Cph1-N515 from *Synechocystis* 6803 have been investigated by NMR spectroscopy, using specific <sup>13</sup>C isotope substitutions in the chromophore. <sup>13</sup>C-NMR spectroscopy in the Pfr and Pr states indicated reversible chemical shift differences predominantly of the C<sub>4</sub> carbon in ring A of the phycocyanobilin chromophore, in contrast to differences of C<sub>15</sub> and C<sub>5</sub>, which were much less pronounced. Ab initio calculations of the isotropic shielding and optical transition energies identify a region for C<sub>4</sub>-C<sub>5</sub>-C<sub>6</sub>-N<sub>2</sub> dihedral angle changes where deshielding of C<sub>4</sub> is correlated with red-shifted absorption. These could occur during thermal reactions on microsecond and millisecond timescales after excitation of Pr which are associated with red-shifted absorption. A reaction pathway involving a hula-twist at C<sub>5</sub> could satisfy the observed NMR and visible absorption changes. Alternatively, C<sub>15</sub> Z-E photoisomerization, although expected to lead to a small change of the chemical shift of C<sub>15</sub>, in addition to changes of the C<sub>4</sub>-C<sub>5</sub>-C<sub>6</sub>-N<sub>2</sub> dihedral angle could be consistent with visible absorption changes and the chemical shift difference at C<sub>4</sub>. NMR spectroscopy of a <sup>13</sup>C-labeled chromopeptide provided indication for broadening due to conformational exchange reactions in the intact photoreceptor domain, which is more pronounced for the C- and D-rings of the chromophore. This broadening was also evident in the F2 hydrogen dimension from heteronuclear <sup>1</sup>H-<sup>13</sup>C HSQC spectroscopy, which did not detect resonances for the <sup>13</sup>C<sub>5</sub>-H, <sup>13</sup>C<sub>10</sub>-H, and <sup>13</sup>C<sub>15</sub>-H hydrogen atoms whereas strong signals were detected for the <sup>13</sup>C-labeled chromopeptide. The most pronounced <sup>13</sup>C-chemical shift difference between chromopeptide and intact receptor domain was that of the <sup>13</sup>C<sub>4</sub>-resonance, which could be consistent with an increased conformational energy of the C<sub>4</sub>-C<sub>5</sub>-C<sub>6</sub>-N<sub>2</sub> dihedral angle in the intact protein in the Pr state. Nuclear Overhauser effect spectroscopy experiments of the <sup>13</sup>C-labeled chromopeptide, where chromophore-protein interactions are expected to be reduced, were consistent with a ZZZssa conformation, which has also been found for the biliverdin chromophore in the x-ray structure of a fragment of *Deinococcus radiodurans* bacteriophytochrome in the Pr form.
- [AQ2]**

## INTRODUCTION

Phytochromes are red and far red light receptors in plants and cyanobacteria that have various physiological roles (2,3). The fundamental spectroscopic changes, which are associated with receptor activation, are similar in most kinds of phytochromes. A red light (~650 nm) absorbing state, called “Pr”, is transformed with relatively low quantum yield (10%) into a far red-absorbing “Pfr” form, which can be retransformed with similar quantum yield using far red light (~710 nm) (4–8). An exception is the biliverdin-containing bacteriophytochrome PPR from *Rhodospirillum centenum*, which has strongly overlapping Pr and Pfr absorption spectra with maxima at 702 nm but with a lower extinction for the Pfr state (9). The Pr states of most phytochromes and bacteriophytochromes (Bphs) are thermally the most stable forms, as has also been found for the cyanobacteriophytochrome Cph1 from *Synechocystis* 6803 (10). This observation has been cited in relation to the expected ZZZ (C<sub>4</sub>,C<sub>10</sub>,C<sub>15</sub>) conformation of all three bridging carbon atoms of the linear tetrapyrrole chromophores of phytochromes (11). In particular, free tetrapyrrole compounds such as phycocyanobilin are known to

adopt helical ZZZ conformations in solution (12–16). However, the biliverdin-containing bacteriophytochrome AtBphP2 from *Agrobacterium tumefaciens* thermally relaxes to a Pfr-like ground state in the dark (17), as do also other bacteriophytochromes (18,19), indicating that the lowest energy conformation available to the free tetrapyrrole chromophores does not necessarily dictate the thermally most stable conformation when bound to phytochrome light receptors.

The phototransformation from the Pr state to the Pfr state has been proposed to involve a Z→E isomerization at the C<sub>15</sub>=C<sub>16</sub> bond between the C- and D-rings of the linear tetrapyrrole chromophore (20–22). Time-resolved and low temperature trapping experiments are consistent with an initial photoisomerization reaction of both Pr and Pfr, followed by a number of slow thermal reactions. Cph1 shows optical and kinetic properties which are representative for many phytochromes, which include a slightly red-shifted lumi-R photoproduct of Pr formed 100 ps after excitation (8). Five subsequent kinetic components are observable on slower timescales ( $\tau_1$ – $\tau_5$ : 5 and 300  $\mu$ s and 3, 30, and 300 ms), which together are responsible for the red-shifted absorption of the Pfr product state (7). Similarly, low temperature trapping of the initial photoproduct lumi-R of Pr below 210 K produced less red-shifted absorption compared to the high temperature result (23). Transient and steady-state protonation studies

Submitted March 1, 2006, and accepted for publication May 17, 2006.

Address reprint requests to Jasper J. van Thor, Laboratory of Molecular Biophysics, University of Oxford, Rex Richards Building, South Parks Road, Oxford OX1 3QU, UK. Tel.: 44-0-1865-285352; Fax: 44-0-1865-275182; E-mail: jasper@biop.ox.ac.uk.

© 2006 by the Biophysical Society

0006-3495/06/09/1/12 \$2.00

doi: 10.1529/biophysj.106.084335

showed that the chromophore is fully protonated in both Pr and Pfr states (7). Therefore, the thermal transformations producing red-shifted products which occur on microsecond and millisecond timescales are likely to result from chromophore configurational changes, additionally considering that many phytochromes show similar spectroscopic and kinetic properties despite having different amino acid sequences.

NMR experiments suggested that a chromopeptide prepared from oat phytochrome in the Pfr form has the C<sub>15</sub>-E configuration, whereas a peptide derived from the Pr form has a C<sub>15</sub>-Z configuration (20). Resonance Raman spectroscopy has identified a strong peak of Pfr at 820 cm<sup>-1</sup> belonging to the C<sub>15</sub>-H hydrogen out of plane mode, which was argued to be consistent with a nonplanar conformation of the C- and D-rings in the Pfr state and supporting the C<sub>15</sub>=C<sub>16</sub> Z→E isomerization (21). A similar mode was identified in the spectra of Cph1 as well, suggesting the same reaction model (22). Calculations of Raman frequencies and intensities of molecular models of the phytychromobilin chromophore of oat phytochrome have refined this reaction model further and invoke an initial ZZZasa (C<sub>4</sub>-Z, C<sub>10</sub>-Z, C<sub>15</sub>-Z, C<sub>5</sub>-anti, C<sub>10</sub>-syn, C<sub>15</sub>-anti) to ZZEasa photoisomerization of Pr transition to the lumi-R photocycle intermediate, followed by a partial thermal ZZEasa to ZZEsa C<sub>5</sub>-C<sub>6</sub> bond rotation producing the Pfr state (24–26). Recently the x-ray structure of a fragment of *Deinococcus radiodurans* bacteriophytochrome DrBphP was reported in the Pr state with the biliverdin chromophore modeled in the ZZZssa conformation (1). Evidence for C<sub>15</sub> Z-E photoisomerization from this structure includes the proximity between Tyr-167 and the D-ring of the chromophore, which in the homologous cyanobacterial phytochrome Cph1 was shown to abolish Pr phototransformation and increase the fluorescence quantum yield when mutated to histidine (27). Here, we use <sup>13</sup>C direct detection NMR spectroscopy of cyanobacterial phytochrome Cph1 with <sup>13</sup>C-labeled phytycyanobilin chromophore to probe the structural changes associated with the Pr to Pfr transition and discuss reaction models that would be consistent with the nuclear magnetic shielding and transient and stable absorption changes.

## MATERIALS AND METHODS

### Sample preparation and NMR spectroscopy

A fragment containing the 515 N-terminal amino acid residues of Cph1 from *Synechocystis* 6803 (Cph1-N515), kindly provided by J. Clark Lagarias, was expressed together with heme oxygenase and bilin reductase, as previously described (28), following a similar procedure (29). A *hemA* aminolevulinic acid auxotrophic BL21(DE3) strain lacking the glutamyl-tRNA reductase gene (30) was used together with 0.5 mM 5-aminolevulinic-5-<sup>13</sup>C acid (Isotec) in the expression medium for the expression of <sup>13</sup>C-labeled material, as described previously (28). The resulting holo Cph1-N515 was isotopically labeled at C<sub>4</sub>, C<sub>5</sub>, C<sub>9</sub>, C<sub>10</sub>, C<sub>11</sub>, C<sub>15</sub>, and C<sub>19</sub> (Fig. 1), and no unlabeled material could be detected using mass spectrometry. The labeling pattern resulting from the heme biosynthesis pathway has been established (28,31–33). Globally <sup>15</sup>N-labeled material was prepared as described previously (28).

Intact protein was purified and used at 200-μM concentration in 4 mM deuterated Tris/HCl pH 7.8, 10% D<sub>2</sub>O. Protein concentration was estimated

using an extinction coefficient of 85 mM<sup>-1</sup> cm<sup>-1</sup> at 655 nm after saturating illumination with far red light (>710 nm) (7,34). NMR spectroscopy of the Pr/Pfr mixed state was performed after saturating illumination with 640-nm light of the concentrated sample in a capillary. Visible spectroscopy of NMR samples after data acquisition confirmed the presence of ~50% of the Pfr state remaining even after several days, due to some dark reversion, in agreement with previous results obtained at lower concentration (10). Illumination of the NMR sample with far red light (>710 nm) produced the stable Pr form. A chromopeptide was prepared starting with the Pr/Pfr-mixed state by digesting Cph1-N515 at 200 μM with 5 μg/mL trypsin for 20 h, which was partially purified by repeated centrifugation and washing of the pellet in water. Mass spectrometry could not determine the mass of the chromopeptide, which was estimated at ~5 kDa from sodium dodecyl sulfate-polyacrylamide gel electrophoresis and <sup>1</sup>H-NMR spectroscopy. The chromopeptide was dissolved in a volume identical to the starting volume in 10% dimethylsulfoxide (DMSO)-d<sub>6</sub>, 10% D<sub>2</sub>O, and 0.1% (w/v) HCl.

All NMR spectra were recorded on a Varian (Palo Alto, CA) UNITY INOVA 500 (<sup>1</sup>H-frequency of 500 MHz, <sup>13</sup>C-frequency of 125 MHz) with a probe temperature of 23°C for intact protein or 25°C chromopeptide samples. A <sup>1</sup>H-<sup>15</sup>N transverse relaxation optimized spectroscopy-heteronuclear single quantum correlation (TROSY-HSQC) spectrum was recorded on uniformly <sup>15</sup>N-labeled intact protein. One-dimensional <sup>13</sup>C-NMR spectra were recorded on the unlabeled and <sup>13</sup>C-labeled intact protein and chromopeptide with broadband <sup>1</sup>H-decoupling, a spectral width of 31.4 KHz, a recycle delay of 2 s, and collecting 230,000 scans. Spectra shown were processed with a 10-Hz exponential line-broadening function, whereas line widths were fitted using spectra that were not processed with apodisation. Two-dimensional <sup>1</sup>H-<sup>13</sup>C HSQC spectra were recorded on both the <sup>13</sup>C-labeled intact protein and chromopeptide. Two-dimensional nuclear Overhauser effect spectroscopy (NOESY) spectra were recorded on the <sup>13</sup>C-labeled chromopeptide using a 400-ms mixing time, 512 complex points in t<sub>1</sub>, and 124 scans per t<sub>1</sub> increment and processed using unshifted cosine-bell functions in both dimensions. A <sup>13</sup>C refocusing pulse was used during the t<sub>1</sub> delay, with or without <sup>13</sup>C-decoupling during t<sub>2</sub>. Thus, <sup>1</sup>Hs attached to <sup>13</sup>C appeared as a singlet in F1 and either a singlet or doublet in F2. A three-dimensional <sup>1</sup>H-<sup>13</sup>C NOESY-HSQC was attempted on the <sup>13</sup>C-labeled chromopeptide, but the signal/noise ratio was too poor for use.

### Computational details

A molecular model for the phycocyanobilin chromophore in the ZZZasa geometry was taken from the 1.45-Å resolution x-ray structure of C-Phycocyanin from *Synechococcus elongates*, PDB 1JBO (35) from the protein data bank. (36) A ZZZssa phycocyanobilin model was based on the ZZZssa biliverdin structure of the *D. radiodurans* bacteriophytochrome fragment, PDB 1ZTU (1). The sulfur linkage was replaced with a hydrogen atom, and all pyrrole nitrogen atoms were protonated. The propionate carboxyl groups were replaced with hydrogen atoms. All calculations were performed using Gaussian 03 (37). In vacuo DFT (38,39) geometry optimization calculations, GIAO isotropic chemical shielding calculations (40–43), and TDDFT excited state calculations (44,45) of the cation models were all performed at the DFT MPW1PW91 6-31G(d,p) level (46). All isotropic shielding calculations are given relative to the values calculated for tetramethylsilane (TMS) calculated at the same level of theory. TDDFT results given are the lowest lying transition energies with significant oscillator strengths, which in all cases provided the isolated HOMO-LUMO transition.

## RESULTS

### <sup>13</sup>C-NMR direct detection of labeled chromophore in intact Cph1-N515 and chromopeptide

Of the C<sub>4</sub>, C<sub>5</sub>, C<sub>9</sub>, C<sub>10</sub>, C<sub>11</sub>, C<sub>15</sub>, and C<sub>19</sub> carbon atoms replaced with <sup>13</sup>C isotopes, only the bridging C<sub>5</sub>, C<sub>10</sub>, and C<sub>15</sub> methine carbons have hydrogen atoms attached (Fig. 1). <sup>13</sup>C

[AQ4]

[AQ5]

[AQ6]

[AQ7]

[AQ8]

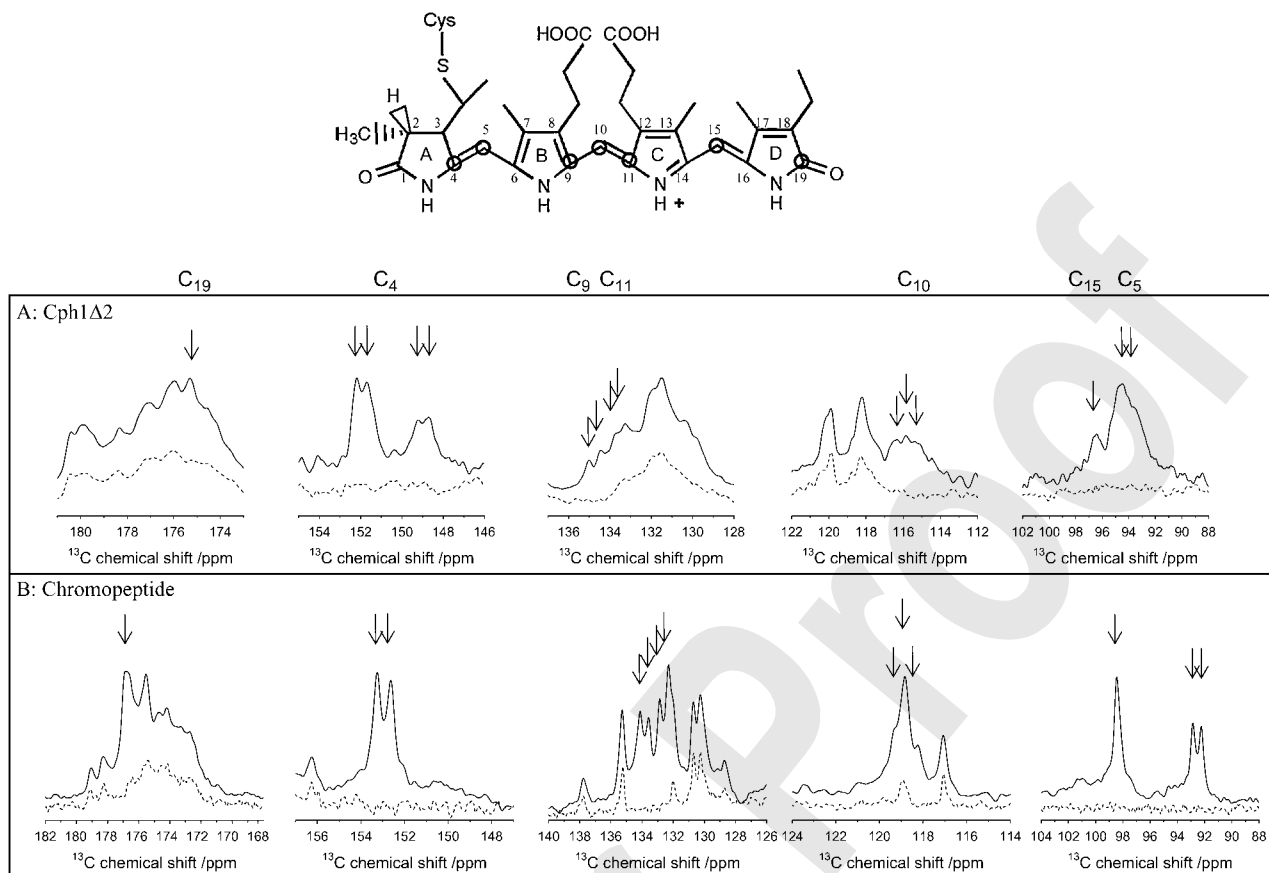


FIGURE 1  $^1\text{H}$ -broadband decoupled  $^{13}\text{C}$ -NMR spectra of labeled (solid lines) and unlabeled (dashed lines) intact Cph1-N515 (A) and chromopeptide (B) identify signals belonging to  $^{13}\text{C}_4$ ,  $^{13}\text{C}_5$ ,  $^{13}\text{C}_9$ ,  $^{13}\text{C}_{10}$ ,  $^{13}\text{C}_{11}$ ,  $^{13}\text{C}_{15}$ , and  $^{13}\text{C}_{19}$ . Labeled and unlabeled Cph1-N515 and derived chromopeptides were at 200- $\mu\text{M}$  concentration, and spectra shown for comparison are not scaled in intensity.

direct detection of intact protein in the mixed Pr and Pfr state with labeled chromophore showed a series of broad peaks in addition to the broad envelope of superimposed signals at natural abundance of the unlabeled 58-kDa polypeptide. For the intact protein the peak widths were 30–40 Hz, typical of resonances of high molecular mass compounds, whereas chromopeptide peak widths were  $\sim 15$  Hz. From the expected dominant  $^{13}\text{C}$ - $^1\text{H}$  dipolar interactions, contributions to the line widths could correspond to rotational correlation times in the order of 30 ns and 12 ns, respectively (47). Comparison of the  $^{13}\text{C}$ -spectra of unlabeled and labeled protein was required to unambiguously identify the peaks belonging to the phycocyanobilin chromophore (Fig. 1 A). Assignment of the peaks was aided by isotropic chemical-shielding calculations (see below) and substantiated by the multiplicity and  $^1\text{J}_{\text{CC}}$ -coupling analysis, which was in agreement with local bond orders (Table 1) and previously published assignments of bilin compounds (14).

### The chromophore is in intermediate conformational exchange in both the Pr and Pfr forms in the intact Cph1-N515 sample

$^1\text{H}$ - $^{13}\text{C}$  HSQC spectra of isotopically labeled Cph1-N515 failed to show crosspeaks for the  $^{13}\text{C}_5$ -H-,  $^{13}\text{C}_{10}$ -H-, and

$^{13}\text{C}_{15}$ -H-chromophore hydrogens, in agreement with a recent study (48). The possibility of paramagnetic contamination was excluded from electron paramagnetic resonance spectroscopy at cryogenic temperature and by proton-induced x-ray emission (MicroPIXE) measurements (not shown). Aggregation was similarly excluded from the line widths of  $^1\text{H}$ -NMR spectra. In the range between 100  $\mu\text{M}$  and 1 mM, no significant changes in line widths of the  $^1\text{H}$ -NMR

TABLE 1  $^{13}\text{C}$ -NMR parameters for the intact protein and the chromopeptide

	Intact (mult; $J_{\text{CC}}$ )/ppm (/Hz)	Chromopeptide (mult; $J_{\text{CC}}$ ) ppm/(/Hz)	Chromopep— Intact/ppm
C <sub>19</sub>	175.3 (s)	177 (s)	+1.5
C <sub>4</sub> (Pfr)	151.9 (d; 65)		
C <sub>4</sub> (Pr)	148.9 (d; 74)	152.9 (d; 81)	+4.0
C <sub>9</sub>	134.7 (d; 70)	133.8 (d; 72)	-0.9
C <sub>11</sub>	133.5 (d; 61)	132.6 (d; 70)	-0.9
C <sub>10</sub>	115.8 (t; 60)	118.8 (t; 71)	+3.0
C <sub>15</sub>	96.5 (s)	98.5 (s)	+2.0
C <sub>5</sub>	94 (d; 60)	92.5 (d; 79)	-1.5

$^{13}\text{C}$ -NMR chemical shifts are reported relative to TMS. Multiplicities and  $J_{\text{CC}}$  values are given in brackets.

spectra of Cph1-N515 were observed, which could be characteristic of a monomeric, or of a rapidly exchanging dimeric, 58-kDa polypeptide. For both Pr and Pfr, concentrations used were in excess of homodimerization dissociation constants reported, (49) but line widths were less than expected for the rigid dimer. Therefore no light-induced changes of populations are expected, which is also corroborated by the similar  $^{13}\text{C}$  line widths in both Pr and Pfr states (Fig. 1). After trypsin digestion of the  $^{13}\text{C}$ -labeled receptor, the same sample at identical concentration showed strong doublet, triplet, and singlet peaks, for the  $^{13}\text{C}_5\text{-H}$ -,  $^{13}\text{C}_{10}\text{-H}$ -, and  $^{13}\text{C}_{15}\text{-H}$ -protons, with  $^1\text{H}$  chemical shifts of 5.55, 7.22, and 6.15 ppm, respectively, whereas no peaks were observed in unlabeled material at the same concentration (Fig. 2, B and

D). The multiplicity and  $^1J_{\text{CC}}$  couplings of the observed peaks matched those that were determined from the  $^{13}\text{C}$ -NMR experiments (Figs. 1 and 2; Table 1). The one-dimensional  $^{13}\text{C}$ -spectra showed that the resonances of, in particular,  $\text{C}_{15}$  and  $\text{C}_{10}$  increased multiplefold in intensity relative to the peptide peaks upon digestion with trypsin (Fig. 2, A and C). This was also observed for the  $\text{C}_4$ ,  $\text{C}_5$ ,  $\text{C}_9$ ,  $\text{C}_{11}$ , and  $\text{C}_{19}$  peaks (not shown) and was most pronounced for the  $\text{C}_{15}$  and least pronounced for the  $\text{C}_5$  peak (Fig. 2 A).  $^1\text{H}$  and  $^1\text{H}$ - $^{15}\text{N}$  TROSY-HSQC spectra of intact  $^{15}\text{N}$  globally labeled Cph1 $\Delta$ 2 at the same concentration were characteristic of a 58-kDa monomeric polypeptide, but the heteronuclear experiment showed considerable broadening of selected resonances (not shown). Together, the data are consistent with the

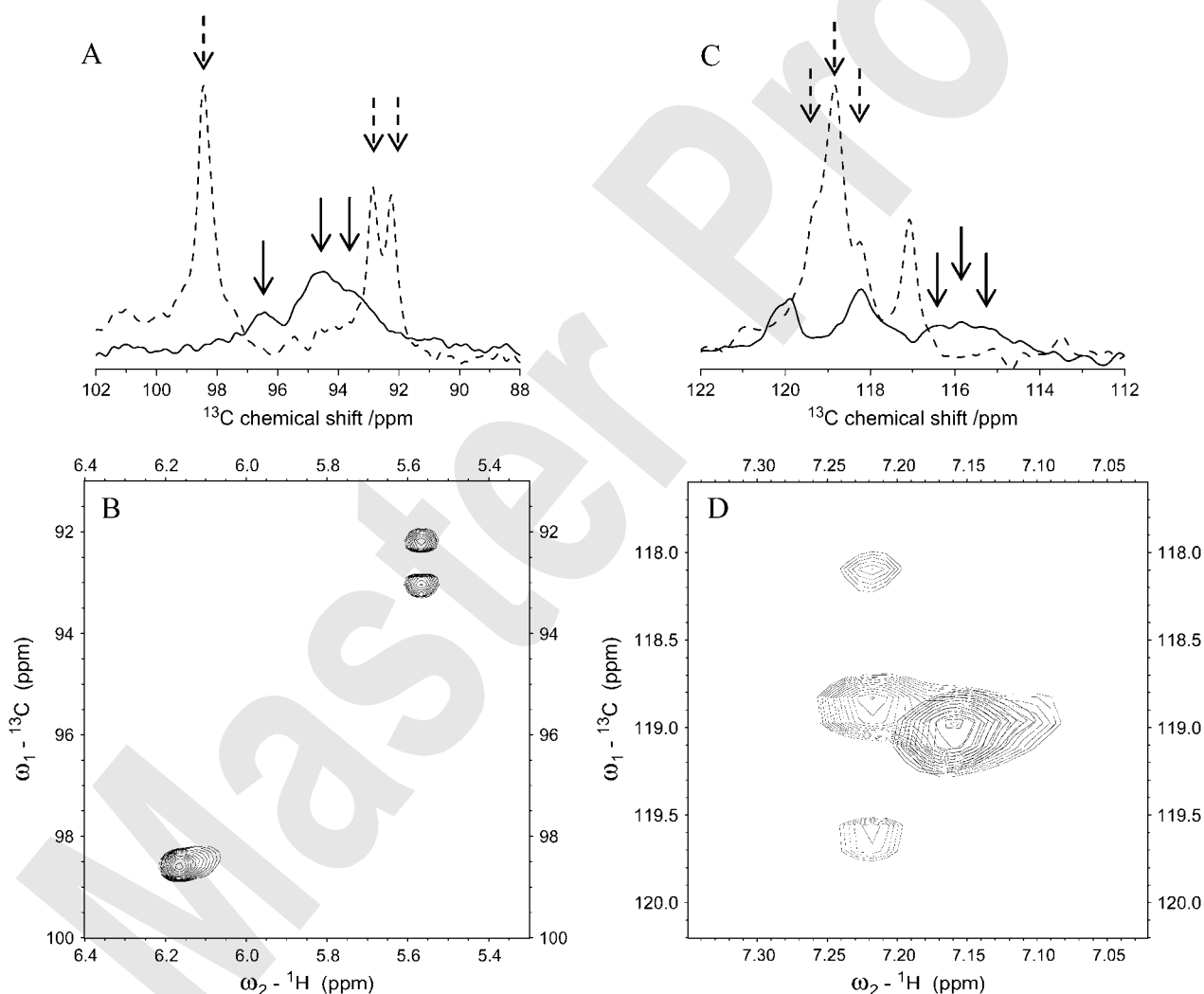


FIGURE 2 Conformational exchange reactions of the chromophore in the intact protein. (A)  $^{13}\text{C}$ -NMR spectra of the  $^{13}\text{C}_5$  and  $^{13}\text{C}_{15}$  carbons in Cph1-N515 (solid line) and chromopeptide (dashed line) under identical experimental conditions and concentration. Arrows indicate chromophore peaks. (B)  $^1\text{H}$ - $^{13}\text{C}$  HSQC crosspeaks for the  $^{13}\text{C}_5\text{-H}$  and  $^{13}\text{C}_{15}\text{-H}$  protons in the labeled chromopeptide. No peaks were observed in this region in unlabeled chromopeptide under identical conditions. (C)  $^{13}\text{C}$ -NMR spectra of the  $^{13}\text{C}_{10}$  triplet in Cph1-N515 (solid line) and chromopeptide (dashed line), indicated with arrows. (D)  $^1\text{H}$ - $^{13}\text{C}$  HSQC crosspeaks of the  $^{13}\text{C}_{10}\text{-H}$  triplet in the labeled chromopeptide (light contours) shown together with the unlabeled chromopeptide, which shows contributions from superimposed resonances at natural abundance in this region (dark contours).

presence of equilibrium conformational exchange reactions in the chromophore in the intact protein on the timescale of the carbon and proton or nitrogen resonance frequency changes accompanying the reaction. The exchange effect was notable in the  $^{13}\text{C}$ -spectra and therefore inferred in  $^1\text{H}$  and  $^{15}\text{N}$  experiments. This broadening of the chromophore resonances in the intact protein is less pronounced proximal to the covalent attachment site at C3', indicating that the change in frequency of these resonances is smaller, leading to faster exchange.

### The chromopeptide-bound phycocyanobilin chromophore is in the ZZZssa conformation

To determine the molecular geometry of the phycocyanobilin chromophore in the chromopeptide, NOESY spectra were recorded on the  $^{13}\text{C}$ -labeled material. Crosspeaks were seen between the  $\text{C}_5$ - $^1\text{H}$ -resonance, observed in these experiments at 5.68 ppm, and peaks at 2.02, 3.18, and 3.35 ppm, assigned to  $\text{C}_7$ - $^1\text{H}$ ,  $\text{C}_3$ - $^1\text{H}$ , and  $\text{C}_3'$ - $^1\text{H}$ , respectively (Fig. 3). The  $\text{C}_{15}$ - $^1\text{H}$ -resonance at 6.29 ppm showed a strong crosspeak to a resonance at 2.14 ppm, assigned either to  $\text{C}_{13}$ - $^1\text{H}$  or  $\text{C}_{17}$ - $^1\text{H}$  (Fig. 3). The 2.14-ppm resonance consists of two closely spaced peaks, with a separation of 8 Hz (Fig. 3), very similar to the peak shapes of the three methyl resonances at 2.02, 2.08, and 2.14 ppm in purified phycocyanobilin in pyridine (not shown). The origin of this peak doubling is uncertain but could be due to *gauche* and anti-*gauche* conformations and is observed in purified phycocyanobilin as well as in the chromopeptide spectra. The chromopeptide spectra therefore did not indicate heterogeneity beyond that observed for the purified chromophore.

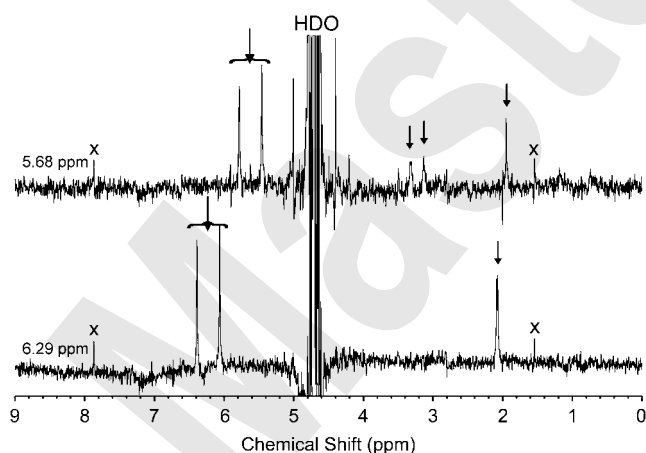


FIGURE 3  $^1\text{H}$ - $^1\text{H}$ -NOESY traces parallel to F2 at 5.68 and 6.29 ppm of the  $^{13}\text{C}$ -labeled chromopeptide. NOESY experiment was run without  $^{13}\text{C}$ -decoupling in F2 to demonstrate the  $J_{\text{CH}}$  coupling in the  $\text{C}_5$ -H and  $\text{C}_{15}$ -H bonds. The brackets and arrows indicate the position of collapsed diagonal peaks as seen in fully decoupled experiments. Artifacts are marked with "X", and NOE crosspeaks are marked with small arrows.

### Pr to Pfr phototransformation results in decreased shielding of $\text{C}_4$

Illumination of Cph1-N515 with far red light produces the pure Pr state, which is the stable form in the dark. Subsequent illumination of NMR samples in thin capillaries with 640-nm light re-forms the Pfr state, which is metastable for several days under conditions used for  $^{13}\text{C}$  direct detection (see Materials and Methods; (10)). Repeated Pr  $\rightarrow$  Pfr and Pfr  $\rightarrow$  Pr phototransformations confirmed reversible changes in the frequency of the  $^{13}\text{C}_4$ -carbon resonance (Fig. 4). In the mixed Pr/Pfr state two doublets are visible for the  $^{13}\text{C}_4$ -carbon, at 151.9 and 148.9 ppm, respectively, whereas after illumination with far red light, only the doublet at 148.9 ppm is observed and increases in intensity (Fig. 4). Changes of the other peaks are much less pronounced. A possible reduction in intensity and perhaps change in frequency of the  $^{13}\text{C}_5$ -doublet at 94 ppm is observed, whereas no change is observed for the frequency of the  $^{13}\text{C}_{15}$ -resonance at 96 ppm. A small reduction in the intensities of peaks belonging to  $^{13}\text{C}_9$ ,  $^{13}\text{C}_{10}$ ,  $^{13}\text{C}_{11}$ ,  $^{13}\text{C}_{15}$ , and possibly  $^{13}\text{C}_{19}$  in the Pr state relative to the Pfr state (not shown) may indicate a change in conformational dynamics.

## DISCUSSION

### Conformational exchange reactions and protein interaction of the chromophore

The conformational exchange reactions of the intact photo-receptor domain hampered  $^1\text{H}$ - $^{13}\text{C}$  HSQC spectroscopy, but resonances for the seven carbons labeled with  $^{13}\text{C}$  could be observed by  $^{13}\text{C}$ -NMR spectroscopy. Line broadening was observed beyond that expected from slow tumbling, manifested by a much reduced intensity relative to chromopeptide resonances at the same concentration. MicroPIXE (50) measurements and ESR spectroscopy at ambient and cryogenic temperatures confirmed that the broadening in the intact protein is not caused by paramagnetic contamination, and aggregation of the intact receptor was also excluded from  $^1\text{H}$ -NMR spectra. Additionally, the increased broadening was removed by proteolytic digestion of the intact material. Hence, conformational exchange reactions are occurring that affect the line width mostly in the  $^1\text{H}$ - but also in the  $^{13}\text{C}$ -frequency domain.

Trypsin digestion removed conformational exchange broadening of the chromophore resonances and strong  $^1\text{H}$ - $^{13}\text{C}$  HSQC crosspeaks were subsequently observed for the  $\text{C}_5$ -H,  $\text{C}_{10}$ -H, and  $\text{C}_{15}$ -H chromophore atoms (Fig. 2). The pronounced gain of intensity of, in particular, the  $^{13}\text{C}_{15}$ -carbon resonance after trypsin digestion suggests that the exchange broadening in the intact protein is greatest at the D-ring end of the molecule. This indicates that the conformational change results in larger changes in chemical shift at the D-ring (these resonances are thus in intermediate exchange) and smaller changes in chemical shift at the

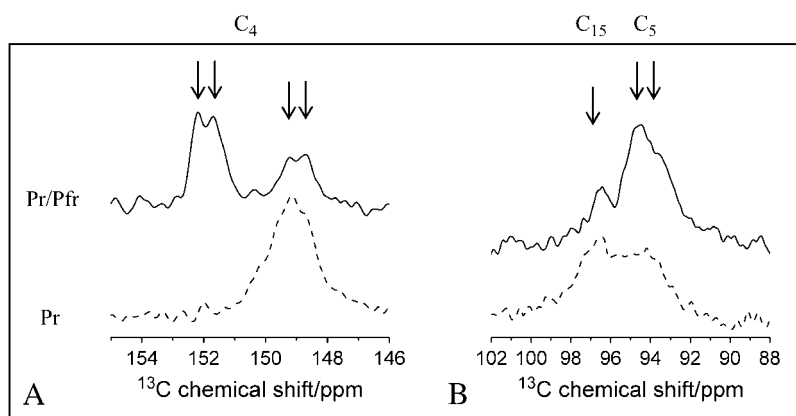


FIGURE 4  $^{13}\text{C}$ -NMR spectroscopy of Pr and Pfr states. The Pr state was obtained in pure form after saturating illumination with  $>705$  nm far red light. A mixture of Pfr and Pr states was obtained after illumination of the concentrated sample in a thin capillary with red light, 640 nm.

A-ring end of the molecule (thus in faster exchange). We note that the binding site proximal half, comprising rings A and B, with the exception of  $\text{C}_4$  become deshielded upon interacting with the protein, whereas the distal end, comprising rings C and D, becomes more shielded (Table 1). The chromopeptide sample contains 10%  $\text{DMSO-d}_6$ , which may contribute to some of the chemical shift changes, but the general trend is noteworthy. We speculate that aromatic stacking on the distal end of the chromophore causes the shielding effect. The conformational exchange of the chromophore observed by NMR spectroscopy may be directly related to the temperature dependence of fluorescence of Cph1, which was interpreted to reflect conformational heterogeneity (51). Additionally, multiple decay phases of the picosecond absorption changes with excitation of the Pr state of Cph1 was interpreted in terms of heterogeneity, or substates, by fitting a distribution of rate constants to the data (8). Conformational exchange reactions of parts of the polypeptide was also observed by  $^1\text{H}$ - $^{15}\text{N}$  TROSY-HSQC spectroscopy of uniformly  $^{15}\text{N}$ -labeled intact Cph1-N515, which showed broadening of a substantial portion of the amide resonances (not shown). The slow conformational exchange reactions which are occurring in the intact material, but not in the digested material, strongly affect the NMR spectroscopy observations and to some extent possibly also the optical properties. The occurrence of closely lying ground state conformations which are separated by thermal barriers result from chromophore-protein interactions which may also affect the phototransformation properties of the intact receptor.

### ZZZssa chromophore conformation in the chromopeptide

The observed NOESY peaks from the  $\text{C}_5$ -H proton in the  $^{13}\text{C}$ -labeled chromopeptide dictate a  $\text{C}_4$ -Z,  $\text{C}_5$ -syn conformation, which fixes the relative positions of rings A and B. The observed single nuclear Overhauser effect (NOE) between  $\text{C}_{15}$ -H and either, but not both, the methyl protons

on rings C or D dictates either a  $\text{C}_{14}$ -anti,  $\text{C}_{15}$ -Z or a  $\text{C}_{14}$ -syn,  $\text{C}_{15}$ -E conformation. Considering the possible  $\text{C}_{14}$ -syn,  $\text{C}_{15}$ -E structures, a ZZEsss conformation is not possible for steric reasons, but a ZEEsas structure could be consistent with the NOE data. Considering possible  $\text{C}_{14}$ -anti,  $\text{C}_{15}$ -Z structures, the ZZZssa is most likely to be the lowest energy conformation. The ZZZssa and ZEEsas geometries were optimized using DFT and found to be, respectively, 17 and 67 kJ/mol higher in energy than the most stable ZZZsss conformation for the fully protonated state. Therefore, the ZZZssa conformation is most likely to exist in the chromopeptide, where stabilizing protein interactions are expected to be reduced. This conformation is tentatively supported by the ZZZssa biliverdin conformation, which was found in the x-ray structure of the homologous bacteriophytochrome fragment (1). The ZZZssa structure of the chromopeptide-bound phycocyanobilin at low pH deviates significantly from the helical ZZZsss conformation found for the purified chromophore (14,16).  $^1\text{H}$ ,  $^1\text{H}$ -NOE enhancements were reported for  $\text{C}_2$ -H and  $\text{C}_{18''}$ -H and also for  $\text{C}_2'$ -H and  $\text{C}_{18'}'$ -H, proposed to belong to two separate helical conformations (16). We confirmed the helical ZZZsss conformation of phycocyanobilin in pyridine but from the NOE enhancement observed for  $\text{C}_{18'}'$ -H and  $\text{C}_3''$ -H (not shown). Interestingly, full protonation of 2,3-dihydrobilindiones was reported not to change the ZZZsss helical conformation as determined from rotating frame Overhauser effect spectroscopy experiments (14), whereas full protonation was suggested to induce extended structures such as observed in protein-bound forms (52). Apparently, remaining chromophore-protein interactions in the chromopeptide stabilize the ZZZssa conformation, but this is not necessarily taken as evidence for the conformation in the intact receptor. NMR experiments with the chromopeptide in the first instance substantiate assignments (Fig. 1) and characterize conformational exchange reactions (Fig. 2). Additionally, the ZZZssa conformation gives confidence that chemical shift differences are not likely to arise from gross configurational differences between chromopeptide and intact protein, assuming similar structures in

Cph1 and *DrBphP* (1). Considering the observation that Cph1, like most phytochromes, relaxes to Pr in the dark in addition to the blue-shifted absorption of the chromopeptide and the *ZZZssa* chromophore structure in the *D. radiodurans* bacteriophytochrome *DrBphP* in the Pr state, it is assumed that the Cph1 chromopeptide is in a Pr-like state (Table 1).

### Chromophore conformation and light-induced changes in the intact Cph1-N515 protein

The  $^{13}\text{C}_4$ -resonance shows the largest reversible change in frequency with phototransformation in the intact protein (Fig. 4), which suggests that bond angle changes occur close to  $\text{C}_4$ . In the more upfield region near 95 ppm, where the  $\text{C}_{15}$  and  $\text{C}_5$  resonances are observed, less pronounced changes are visible (Fig. 4). These are interpreted to show an intensity change of the  $\text{C}_5$ -resonance, leaving the  $\text{C}_{15}$ -resonance mostly unchanged. This view would also fit with the observed changes at  $\text{C}_4$ , which shares  $\pi$ -orbital valence electrons with  $\text{C}_5$ . Recent evidence suggests that the initial photoisomerization occurs at the  $\text{C}_{15}=\text{C}_{16}$  bond (24–26,53). One study using sterically locked biliverdin derivatives implied a *Z-anti* and *E-syn* conformation for the  $\text{C}_{15}$ -carbon of the Pr and Pfr states, respectively (53), which has been confirmed for the Pr state of the biliverdin chromophore of *D. radiodurans DrBphP* (1). Persuasive evidence for  $\text{C}_{15}=\text{C}_{16}$  bond photoisomerization is the lack of phototransformation and high fluorescence quantum yield of a Y167H mutant of Cph1 (27), considering that the conserved tyrosine 167 at that position in the homologous *D. radiodurans Bph* is in 4 Å distance of the D-ring (1). Raman spectroscopy studies and mode calculations of phytochromobilin containing oat phytochrome (24,25) and biliverdin-containing Agp1 bacteriophytochrome (26), both concluding that the Pr to Pfr transformation is initiated by a *ZZZasa* to *ZZEasa* photoisomerization followed by a partial *anti* to *syn* thermal  $\text{C}_5\text{-C}_6$  bond rotation.

We note that the NMR data independently suggest bond angle changes at  $\text{C}_5$ .

Ab initio isotropic chemical shielding calculations were performed for *ZZZasa*, *ZZEasa*, and *ZZEssa* chromophore models in vacuum (Table 2). The GAIO calculations consistently indicated that in energy-minimized conformations a  $\text{C}_5$ -*anti* to *-syn* rotation is expected to lead to increased shielding of the  $\text{C}_4$ -carbon atom, in both the  $\text{C}_4\text{-E}$  and  $\text{C}_4\text{-Z}$  configurations (Table 2). This was also confirmed at the GAIO DFT B3LYP 6-311G+(2d,2p), GAIO HF 6-311G+(2d,2p), and CSGT B3LYP cc-PVDZ levels as well as with solvent reaction field modeling using the polarizable continuum method (37). The calculations performed at different levels of theory all indicated similar changes of the  $^{13}\text{C}_4$ -resonance frequency resulting from  $\text{C}_4\text{-C}_5\text{-C}_6\text{-N}_2$  dihedral angle changes. We note that the absolute values of calculated shielding values do not identify conformations, but the differences calculated with bond angle changes are interpreted.

$\text{C}_{15}$  Z-E photoisomerization is calculated to lead an ~2-ppm downfield shift of the  $\text{C}_{15}$ -resonance (Table 2), which was also confirmed for geometry-optimized *ZZZssa* and *ZZEssa* conformations in vacuum as well as for *ZZZssa* and *ZZEssa* phycocyanobilin conformations based on the *D. radiodurans Bph* x-ray structure, by including a 204°  $\text{N}_3\text{-C}_{14}\text{-C}_{15}\text{-C}_{16}$  dihedral angle restraint (Table 2).  $\text{N}_3\text{-C}_{14}\text{-C}_{15}\text{-C}_{16}$  dihedral angle changes would lead to further, more pronounced, chemical shift changes of  $\text{C}_{15}$  (not shown). TDDFT calculations show that  $\text{C}_{15}$  Z-E isomerization could be responsible for red-shifted absorption of the photoproduct but could explain neither the observed  $\text{C}_4$  chemical shift changes (not considering possible environmental rearrangements near ring A) nor the absence of chemical shift changes of  $\text{C}_{15}$  (Table 2). The NMR data and calculations can therefore not easily be reconciled with a  $\text{C}_{15}$  Z-E isomerization in

**TABLE 2** Conformational energies, optical transition energies, and isotropic  $^{13}\text{C}$ -NMR shielding values calculated for several chromophore models

	<i>ZZZssa</i> (1)	<i>ZZEssa</i> (2)	<i>ZZZsss</i>	<i>ZZZasa</i>	<i>ZZEasa</i>	<i>ZZEssa</i>	<i>ZZZssa</i> (3)	<i>EZZssa</i>	<i>EZZasa</i> (4)
Constrained dihedral angle/°	$\text{N}_3\text{-C}_{14}\text{-C}_{15}\text{-C}_{16}$ 204	$\text{N}_3\text{-C}_{14}\text{-C}_{15}\text{-C}_{16}$ 204					$\text{C}_4\text{-C}_5\text{-C}_6\text{-N}_2$ 275	$\text{C}_4\text{-C}_5\text{-C}_6\text{-N}_2$ 275	
energy /kJ/mol	31.1	48.2	0	30.1	52.0	40.3	48.6	58.5	38.9
HOMO → LUMO (oscillator strength)	2.16 eV, 574 nm, $f = 0.82$	2.11 eV, 586 nm, $f = 0.75$	2.04 eV, 607 nm, $f = 0.32$	2.28 eV, 541.7 nm, $f = 1.42$	2.28 eV, 543.1 nm, $f = 1.36$	2.12 eV, 585.9 nm, $f = 0.74$	2.37 eV, 522.5 nm, $f = 0.74$	2.41 eV, 515.0 nm, $f = 0.63$	2.29 eV, 540.9 nm, $f = 1.41$
$\text{C}_{19}$	162.9	161.5	169.3	162.3	161.4	161.3	162.4	162.4	162.4
$\text{C}_4$	154.3	154.1	159.3	157.4	157.9	154.0	153.1	152.7	158.4
$\text{C}_9$	128.5	128.9	127.9	126.5	126.7	129.0	125.0	124.7	126.4
$\text{C}_{11}$	127.6	128.2	126.4	126.6	126.2	127.8	126.8	126.5	126.5
$\text{C}_{10}$	112.0	112.4	110.0	112.8	113.1	113.0	115.6	115.8	112.6
$\text{C}_{15}$	88.2	90.3	92.6	87.0	87.7	89.4	86.7	86.6	87.0
$\text{C}_5$	86.6	86.8	86.2	83.6	83.6	87.4	81.2	81.4	84.8

Dihedral angle restraints used in the geometry optimization are listed, and none were used if not listed. Conformational energies are given relative to the lowest energy *ZZZsss* model. Optical transition energies as calculated by TDDFT are given in eV, with corresponding wavelength, including the oscillator strengths. NMR shielding is reported for all  $^{13}\text{C}$ -labeled chromophore atoms, relative to TMS (ppm). 1), Conformation based on the *D. radiodurans Bph* x-ray structure; 2), *ZZEssa* structure based on 1); 3), structure shown in Fig. 6 C; and 4), structure shown in Fig. 6 D.

the Pr to Pfr photoreaction without additional low order bond rotation(s) at C<sub>5</sub> and possibly C<sub>14</sub>. One note of caution concerns the low intensity of the <sup>13</sup>C<sub>15</sub>-resonance in the intact protein relative to the chromopeptide, which shows that not the entire population is observed in <sup>13</sup>C direct experiments comparing Pr and Pfr states in the intact protein (Fig. 2). Our data therefore do not rule out changes at C<sub>15</sub>, in case its resonance is specifically broadened in the Pfr state as a result of conformational exchange dynamics.

Both fast and slow optical changes in the Pr to Pfr pathway would ideally be reconciled with proposals for the reaction pathway. Notably, the primary photoproduct lumi-R of Pr observed 100 ps after excitation of Cph1 is only slightly red-shifted (8), whereas TDDFT calculations suggest that C<sub>15</sub> Z-E isomerization would lead to a considerable red-shift (Table 2). The optical changes occurring during thermal reactions on microsecond and millisecond timescales after excitation of Pr are responsible for the main absorption difference between Pr and Pfr of Cph1 (7,22), implying that these occur as a result of low order bond rotation(s).

A scan of the C<sub>4</sub>-C<sub>5</sub>-C<sub>6</sub>-N<sub>2</sub> dihedral angle in both the ZZZ(s)sa and EZZ(s)sa was performed, with constrained geometry optimization for each configuration, to compute the <sup>13</sup>C<sub>4</sub>-NMR and optical properties (Fig. 5). These calculations identify a region in the ZZZssa (as well as in the EZZssa) geometry between 275° and 360° (Fig. 6 C) where a decrease of the TDDFT excitation energy is correlated with the deshielding of C<sub>4</sub> (Fig. 5, B and C). In one possible model, C<sub>15</sub> Z-E photoisomerization followed by C<sub>4</sub>-C<sub>5</sub>-C<sub>6</sub>-N<sub>2</sub> dihedral angle rotation between 275° and 360°, or by relaxation of the stretched conformation by reduction of the C<sub>4</sub>-C<sub>5</sub>-C<sub>6</sub> bond angle, might explain the NMR results and possibly the optical and kinetic properties. This reaction model would be very similar to the reaction model proposed on the basis of Raman spectroscopy (24–26). However, the apparent absence of C<sub>15</sub> chemical shift differences and the calculated red-shift of the primary photoproduct are not strongly supportive of this possibility, although conformational exchange and environmental effects may play a role in the NMR and optical properties, respectively.

Alternatively, photoisomerization could occur at C<sub>4</sub>, followed by C<sub>4</sub>-C<sub>5</sub>-C<sub>6</sub>-N<sub>2</sub> dihedral angle rotation. C<sub>4</sub> Z-E photoisomerization with a 275° dihedral angle leads to only very small optical changes, which would be consistent with the slightly red-shifted primary photoproduct lumi-R of Pr observed 100 ps after excitation of Cph1 (8). A thermal activation barrier between 275° (*syn*) and 150° (*anti*) conformations subsequently might separate the lumi-R and the Pfr states, which could be consistent with the red-shifted reaction products which are formed on the microsecond and millisecond timescales after excitation of Pr (7,22). The Z-E isomerization and thermal bond rotation together would constitute a hula-twist motion, which would be more likely given the constraint of covalent attachment of ring A. Cryotrapping of the first metastable “meta-Ra” intermediate

of Pr occurs at 233 K (23), which would be consistent with the existence of a rotational barrier in the reaction pathway. Fluorescence measurements of Cph1 at low temperature indicated that the primary photochemical reactions were inhibited below 170 K (51), which together with the low photochemical quantum yield of phototransformation at ambient temperature indicates the presence of a substantial barrier for the initial photoisomerization reaction. Such a barrier may be the result of conformational restraint of the chromophore via covalent linkage on ring A close to the isomerization site.

The models including specific C<sub>4</sub>-C<sub>5</sub>-C<sub>6</sub>-N<sub>2</sub> dihedral angle changes do not use the conformations with the lowest possible conformational energies as optimized and computed in vacuum in the absence of specific interactions (Fig. 5). The associated energy as determined by DFT calculations is reasonable. In addition, the ZZZssa biliverdin chromophore in the x-ray structure of *D. radiodurans* Bph is present in a higher energy conformation, considering the 204° N<sub>3</sub>-C<sub>14</sub>-C<sub>15</sub>-C<sub>16</sub> dihedral angle and the 130° and 135° methine C<sub>5</sub> and C<sub>10</sub> bridge angles. DFT geometry optimization indicated that ~73 kJ/mol is associated with the stretched conformation as refined from the x-ray data increasing the C<sub>5</sub> and C<sub>10</sub> methine bond angles by more than 10° and 8 kJ/mol with the twisted N<sub>3</sub>-C<sub>14</sub>-C<sub>15</sub>-C<sub>16</sub> dihedral angle. These calculations assume full protonation on all nitrogens also in the case of *D. radiodurans* Bph biliverdin. This stretching also causes chemical shift and optical differences. Geometry optimization using redundant coordinates for the 130° and 135° methine C<sub>5</sub> and C<sub>10</sub> bridge angles indicates a blue-shifted absorption from subsequent TDDFT calculations. Similarly, intermediate configurations taken from the optimization indicate that stretching could be associated with 3 ppm increased shielding of C<sub>4</sub> and a 0.11 eV increase of the TDDFT excitation energy. This stretching, possibly only locally at C<sub>5</sub>, could therefore produce similar NMR and optical changes as C<sub>4</sub>-C<sub>5</sub>-C<sub>6</sub>-N<sub>2</sub> dihedral angle rotation between 275° and 360°. It is possible that conformational stretching and relaxing, rather than low order bond rotations, contribute to the observed NMR and optical changes but in the absence of further molecular information on the Pfr state is not explicitly considered.

## CONCLUSIONS

The reaction models that are discussed aim to satisfy the NMR measurements, as well as the optical and kinetic properties of the phototransformation of Cph1. These neglect effects of specific protein interactions with the chromophore but could provide a generally valid mechanism for the light-induced changes in phytochromes, which have common spectroscopic characteristics despite different polypeptide sequences. The chromophore heterogeneity in the intact receptor domain, which is apparent from the exchange broadening and which is also suggested from fluorescence studies (51), adds additional complexity. Evidence favoring

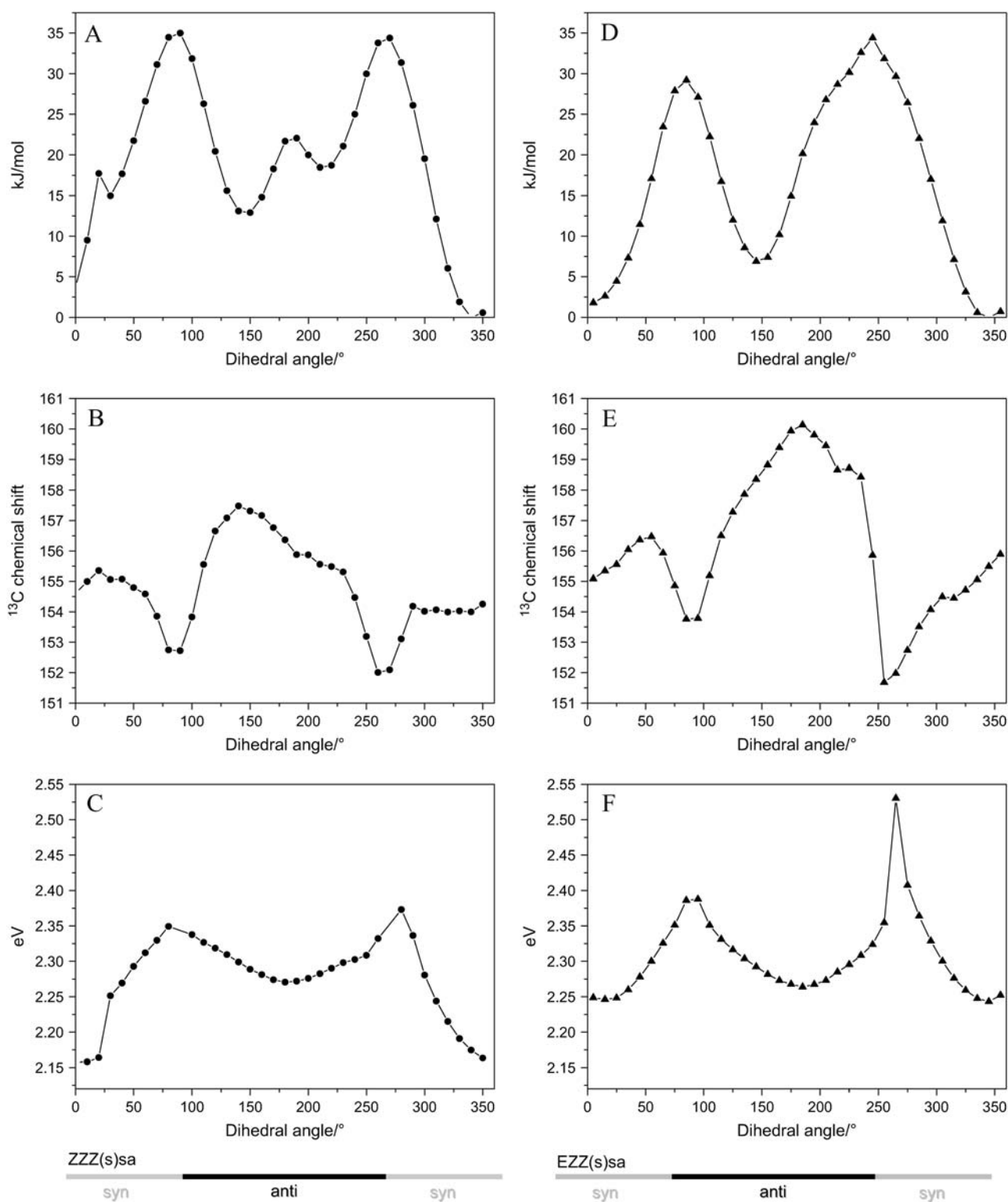


FIGURE 5 Molecular properties with C<sub>4</sub>-C<sub>5</sub>-C<sub>6</sub>-N<sub>2</sub> dihedral angle changes. A relaxed C<sub>4</sub>-C<sub>5</sub>-C<sub>6</sub>-N<sub>2</sub> dihedral angle scan was performed of the ZZZ(s)sa (A-C) (●) and EZZ(s)sa (D-F) (▲) geometries. DFT conformational energies (kJ/mol) (A and D) are given relative to the lowest conformation. Isotropic chemical shielding values are given for the <sup>13</sup>C<sub>4</sub>-carbon relative to TMS (ppm) (B and E). TDDFT optical transition energies computed for the pure HOMO-LUMO transition (eV) (C and F).

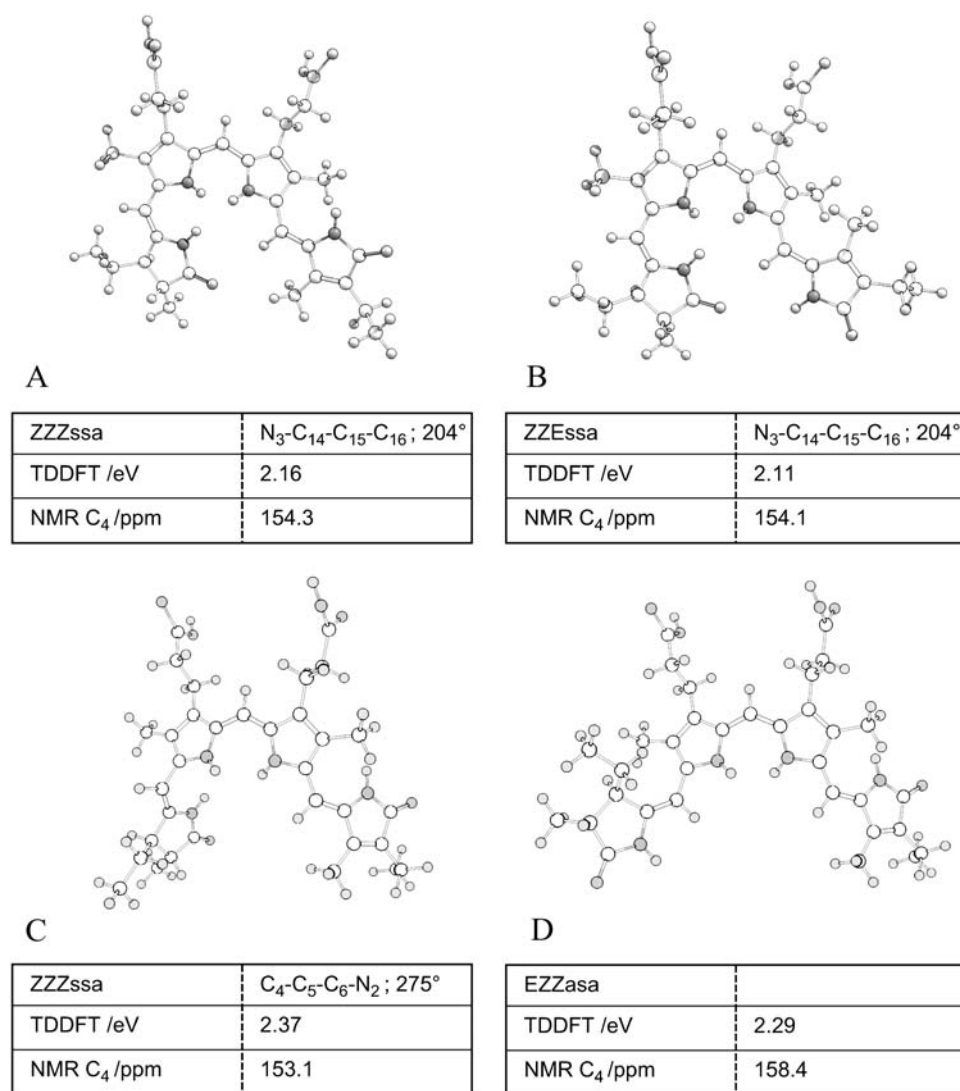


FIGURE 6 Chromophore models and key calculated properties. The conformational models shown are the optimized geometries at the DFT MPW1PW91/6-31G(d,p) level also used for the GAIO and TDDFT calculations but additionally contain the carboxylic acid groups which were excluded in the calculations. Dihedral angle restraints used in the geometry optimization, the calculated isotropic shielding for  $C_4$  and the TDDFT excitation energy are listed as a summary of the results, which are discussed. (A) ZZZssa model obtained after geometry optimization as taken from the Bph x-ray structure. (B) ZZEssa structure based on A. (C) ZZZssa structure including only the  $C_4-C_5-C_6-N_2$  dihedral angle restraint. (D) EZZasa structure based on C.

$C_{15}$  Z-E photoisomerization is taken from the recent x-ray structure of the *D. radiodurans* Bph fragment together with the fluorescent Y167H mutant of Cph1. To satisfy NMR and optical properties, additional  $C_4-C_5-C_6-N_2$  dihedral angle or possibly  $C_4-C_5-C_6$  bond angle changes are expected, supporting details from previous models based on Raman spectroscopy (24–26).  $C_{15}$  Z-E photoisomerization would be expected to lead to rapid optical changes and NMR frequency changes of  $C_{15}$ , both of which are not observed and would have to be explained by environmental tuning effects or twisted  $\pi$ -bond geometry and Pfr state-specific conformational exchange, respectively. Alternatively, a  $C_4$  Z-E photoisomerization and a  $C_5$  *syn-anti* bond rotation could explain the data and might be at the basis of the photoreaction of the cyanobacterial phytochrome Cph1 and also other (bacterio)phytochromes. Since the chromophore is covalently bound to the protein via the  $C_{3'}$  carbon on ring A, hula-twist motions of the  $C_4=C_5$  and  $C_5-C_6$  bonds are perhaps more likely, which future calculations may address.

We thank Timothy Claridge and Jim McDonnell for help and discussion and Clark Lagarias for reading of the manuscript. We thank Jenny Gibson for technical support. We gratefully acknowledge the Oxford Supercomputing facilities, Eric McInnes, and the Engineering and Physical Sciences Research Council Electron Paramagnetic Resonance Research Center facility at Manchester University and the MicroPIXE facility at the University of Surrey, Guildford, UK.

M.M. is supported by a scholarship from the Government of Malaysia. I.K. was supported by the Scatcherd European Foundation and the Hill Foundation. This work was also supported by funding from the Oxford Glycobiology Institute.

J.J.v.T. is a Royal Society University Research Fellow. M.M. is on study leave from Universiti Putra Malaysia.

## REFERENCES

1. Wagner, J. R., J. S. Brunzelle, K. T. Forest, and R. D. Vierstra. 2005. A light-sensing knot revealed by the structure of the chromophore-binding domain of phytochrome. *Nature*. 438:325–331.
2. Montgomery, B. L., and J. C. Lagarias. 2002. Phytochrome ancestry: sensors of bilins and light. *Trends Plant Sci.* 7:357–366.

3. Lamparter, T. 2004. Evolution of cyanobacterial and plant phytochromes. *FEBS Lett.* 573:1–5.
4. Butler, W. L., K. H. Norris, H. W. Siegelman, and S. B. Hendricks. 1959. Detection, assay and preliminary purification of the pigment controlling photoresponsive developments of plants. *Proc. Natl. Acad. Sci. USA.* 45:1703–1708.
5. Kelly, J. M., and J. C. Lagarias. 1985. Photochemistry of 124 kilodalton Avena phytochrome under constant illumination in vitro. *Biochemistry.* 24:6003–6010.
6. Lagarias, J. C., J. M. Kelly, K. L. Cyr, and W. O. Smith Jr. 1987. Comparative photochemical analysis of highly purified 124 kilodalton oat and rye phytochromes in vitro. *Photochem. Photobiol.* 46:5–13.
7. van Thor, J. J., B. Borucki, W. Crielard, H. Otto, T. Lamparter, J. Hughes, K. J. Hellingwerf, and M. P. Heyn. 2001. Light-induced proton release and proton uptake reactions in the cyanobacterial phytochrome Cph1. *Biochemistry.* 40:11460–11471.
8. Heyne, K., J. Herbst, D. Stehlik, B. Esteban, T. Lamparter, J. Hughes, and R. Diller. 2002. Ultrafast dynamics of phytochrome from the cyanobacterium *synechocystis*, reconstituted with phycocyanobilin and phycoerythrobilin. *Biophys. J.* 82:1004–1016.
9. Kyndt, J. A., T. E. Meyer, and M. A. Cusanovich. 2004. Photoactive yellow protein, bacteriophytochrome, and sensory rhodopsin in purple phototrophic bacteria. *Photochem. Photobiol. Sci.* 3:519–530.
10. Yeh, K. C., S. H. Wu, J. T. Murphy, and J. C. Lagarias. 1997. A cyanobacterial phytochrome two-component light sensory system. *Science.* 277:1505–1508.
11. Li, L., and J. C. Lagarias. 1992. Phytochrome assembly. Defining chromophore structural requirements for covalent attachment and photoreversibility. *J. Biol. Chem.* 267:19204–19210.
12. Crespi, H. L., U. Smith, and J. J. Katz. 1968. Phycocyanobilin. Structure and exchange studies by nuclear magnetic resonance and its mode of attachment in phycocyanin. A model for phytochrome. *Biochemistry.* 7:2232–2242.
13. Bishop, J. E., J. O. Nagy, J. F. O'Connell, and H. Rapoport. 1991. Diastereoselective synthesis of phycocyanobilin-cysteine adducts. *J. Am. Chem. Soc.* 118:8024–8035.
14. Stanek, M., and K. Grubmayr. 1998. Protonated 2,3-dihydrobilindiones—Models for the chromophores of phycocyanin and the red-absorbing form of phytochrome. *Chem. Eur. J.* 4:1653–1659.
15. Krois, D. 1991. Geometry versus basicity of bilatrienes: stretched and helical protonated biliverdins. *Monatsh. Chem.* 122:495–506.
16. Knipp, B., M. Müller, N. S. B. Metzler-Nolte, T. S. E. Braslavsky, and K. Schaffner. 1998. NMR verification of helical conformations of phycocyanobilin in organic solvents. *Helv. Chim. Acta.* 81:881–888.
17. Karniol, B., and R. D. Vierstra. 2003. The pair of bacteriophytochromes from *Agrobacterium tumefaciens* are histidine kinases with opposing photobiological properties. *Proc. Natl. Acad. Sci. USA.* 100:2807–2812.
18. Karniol, B., J. R. Wagner, J. M. Walker, and R. D. Vierstra. 2005. Phylogenetic analysis of the phytochrome superfamily reveals distinct microbial subfamilies of photoreceptors. *Biochem. J.* 392:103–116.
19. Giraud, E., J. Fardoux, N. Fourrier, L. Hannibal, B. Genty, P. Bouyer, B. Dreyfus, and A. Vermeglio. 2002. Bacteriophytochrome controls photosystem synthesis in anoxygenic bacteria. *Nature.* 417:202–205.
20. Rudiger, W. T., F. Tummeler, E. Cmiel, and S. Schneider. 1983. Chromophore structure of the physiologically active form Pfr of phytochrome. *Proc. Natl. Acad. Sci. USA.* 80:6244–6248.
21. Andel 3rd, F., J. T. Murphy, J. A. Haas, M. T. McDowell, I. van der Hoef, J. Lugtenburg, J. C. Lagarias, and R. A. Mathies. 2000. Probing the photoreaction mechanism of phytochrome through analysis of resonance Raman vibrational spectra of recombinant analogues. *Biochemistry.* 39:2667–2676.
22. Remberg, A., I. Lindner, T. Lamparter, J. Hughes, C. Kneip, P. Hildebrandt, S. E. Braslavsky, W. Gartner, and K. Schaffner. 1997. Raman spectroscopic and light-induced kinetic characterization of a recombinant phytochrome of the cyanobacterium *Synechocystis*. *Biochemistry.* 36:13389–13395.
23. Foerstendorf, H., T. Lamparter, J. Hughes, W. Gartner, and F. Siebert. 2000. The photoreactions of recombinant phytochrome from the cyanobacterium *Synechocystis*: a low-temperature UV-Vis and FT-IR spectroscopic study. *Photochem. Photobiol.* 71:655–661.
24. Kneip, C., P. Hildebrandt, W. Schlamann, S. E. Braslavsky, F. Mark, and K. Schaffner. 1999. Protonation state and structural changes of the tetrapyrrole chromophore during the Pr → Pfr phototransformation of phytochrome: a resonance Raman spectroscopic study. *Biochemistry.* 38:15185–15192.
25. Mroginski, M. A., D. H. Murgida, D. von Stetten, C. Kneip, F. Mark, and P. Hildebrandt. 2004. Determination of the chromophore structures in the photoinduced reaction cycle of phytochrome. *J. Am. Chem. Soc.* 126:16734–16735.
26. Borucki, B., D. von Stetten, S. Seibeck, T. Lamparter, N. Michael, M. A. Mroginski, H. Otto, D. H. Murgida, M. P. Heyn, and P. Hildebrandt. 2005. Light-induced proton release of phytochrome is coupled to the transient deprotonation of the tetrapyrrole chromophore. *J. Biol. Chem.* 40:34358–34364.
27. Fischer, A. J., and J. C. Lagarias. 2004. Harnessing phytochrome's glowing potential. *Proc. Natl. Acad. Sci. USA.* 101:17334–17339.
28. van Thor, J. J., N. Fisher, and P. R. Rich. 2005. Assignments of the Pfr-Pr FTIR difference spectrum of cyanobacterial phytochrome Cph1 using a 15N and 13C isotopically labelled phycocyanobilin chromophore. *J. Phys. Chem. B.* 109:20597–20604.
29. Gambetta, G. A., and J. C. Lagarias. 2001. Genetic engineering of phytochrome biosynthesis in bacteria. *Proc. Natl. Acad. Sci. USA.* 98:10566–10571.
30. Nakayashiki, T., K. Nishimura, R. Tanaka, and H. Inokuchi. 1995. Partial inhibition of protein synthesis accelerates the synthesis of porphyrin in heme-deficient mutants of *Escherichia coli*. *Mol. Gen. Genet.* 249:139–146.
31. Panek, H., and M. R. O'Brian. 2002. A whole genome view of prokaryotic haem biosynthesis. *Microbiology.* 148:2273–2282.
32. Rivera, M., F. Qiu, R. A. Bunce, and R. E. Stark. 1999. Complete isomer-specific 1H and 13C NMR assignments of the heme resonances of rat liver outer mitochondrial membrane cytochrome b5. *J. Biol. Inorg. Chem.* 4:87–98.
33. Qiu, F., M. Rivera, and R. E. Stark. 1998. An 1H–13C–13C-edited 1H NMR experiment for making resonance assignments in the active site of heme proteins. *J. Magn. Reson.* 130:76–81.
34. Lamparter, T., B. Esteban, and J. Hughes. 2001. Phytochrome Cph1 from the cyanobacterium *synechocystis* PCC6803. Purification, assembly, and quaternary structure. *Eur. J. Biochem.* 268:4720–4730.
35. Nield, J., P. J. Rizkallah, J. Barber, and N. E. Chayen. 2003. The 1.45 Å three-dimensional structure of C-phycocyanin from the thermophilic cyanobacterium *Synechococcus elongatus*. *J. Struct. Biol.* 141:149–155.
36. Berman, H. M., J. Westbrook, Z. Feng, G. Gilliland, T. N. Bhat, H. Weissig, I. N. Shindyalov, and P. E. Bourne. 2000. The protein data bank. *Nucleic Acids Res.* 28:235–242.
37. Frisch, M. J. T. G. W., H. B. Schlegel, G. E. Scuseria, M. A. Robb, J. R. Cheeseman, J. A. Montgomery, T. Vreven, K. N. Kudin, J. C. Burant, J. M. Millam, S. S. Iyengar, J. Tomasi, V. Barone, B. Mennucci, M. Cossi, G. Scalmani, N. Rega, G. A. Petersson, H. Nakatsuji, M. Hada, M. Ehara, K. Toyota, R. Fukuda, J. Hasegawa, M. Ishida, T. Nakajima, Y. Honda, O. Kitao, H. Nakai, M. Klene, X. Li, J. E. Knox, H. P. Hratchian, J. B. Cross, V. Bakken, C. Adamo, J. Jaramillo, R. Gomperts, R. E. Stratmann, O. Yazyev, A. J. Austin, R. Cammi, C. Pomelli, J. W. Ochterski, P. Y. Ayala, K. Morokuma, G. A. Voth, P. Salvador, J. J. Dannenberg, V. G. Zakrzewski, S. Dapprich, A. D. Daniels, M. C. Strain, O. Farkas, D. K. Malick, A. D. Rabuck, K. Raghavachari, J. B. Foresman, J. V. Ortiz, Q. Cui, A. G. Baboul, S. Clifford, J. Cioslowski, B. B. Stefanov, G. Liu, A. Liashenko, P. Piskorz, I. Komaromi, R. L. Martin, D. J. Fox, T. Keith, M. A. Al-Laham, C. Y. Peng, A. Nanayakkara, M. Challacombe, P. M. W. Gill, B. Johnson, W. Chen, M. W. Wong, C. Gonzalez, and J. A. Pople. 2004. Gaussian 03. Gaussian, Inc., Wallingford, CT.

- [AQ11] 38. Hohenberg, P., and W. Khon. 1964. Inhomogeneous electron gas. *Phys. Rev.* 136:B864–B871.
39. Khon, W., and L. J. Sham. 1965. Self-consistent equations including exchange and correlation effects. *Phys. Rev.* 140:A1133–A1138.
40. London, F. 1937. Quantum theory of interatomic currents in aromatic compounds. *J. Phys. Radium.* 8:397–409.
41. Ditchfield, R. 1974. Self-consistent perturbation theory of diamagnetism. I. A gauge-invariant linear combination of atomic orbitals. Method for NMR chemical shifts. *Mol. Phys.* 27:789–807.
42. Wolinski, K., J. F. Hinton, and P. Pulay. 1990. Efficient implementation of the gauge-independent atomic orbital method for NMR chemical shift calculations. *J. Am. Chem. Soc.* 112:8251–8260.
43. Cimino, P., L. Gomez-Paloma, D. Duca, R. Riccio, and G. Bifulco. 2004. Comparison of different theory models and basis sets in the calculation of <sup>13</sup>C NMR chemical shifts of natural products. Magnetic resonance in chemistry. *Magn. Reson. Chem.* 42:S26–S33.
- [AQ12] 44. Bauernschmitt, R., and R. Ahlrichs. 1996. Treatment of electronic excitations within the adiabatic approximation of time-dependent density functional theory. *Chem. Phys. Lett.* 256:454.
- [AQ13] 45. Casida, M. E., C. Jamorski, K. C. Casida, and D. R. Salahub. 1998. Molecular excitation energies to high-lying bound states from time-dependent density-functional response theory: characterization and correction of the time-dependent local density approximation ionization threshold. *J. Chem. Phys.* 108:4439.
46. Adamo, C., and V. Barone. 1998. Exchange functionals with improved long-range behavior and adiabatic connection methods without adjustable parameters: the mPW and mPW1PW models. *J. Chem. Phys.* 108:664. [AQ14]
47. Gardner, K. H., and L. E. Kay. 1998. The use of <sup>2</sup>H, <sup>13</sup>C, <sup>15</sup>N multidimensional NMR to study the structure and dynamics of proteins. *Annu. Rev. Biophys. Biomol. Struct.* 27:357–406.
48. Strauss, H. M., J. Hughes, and P. Schmieder. 2005. Heteronuclear solution-state NMR studies of the chromophore in cyanobacterial phytochrome Cph1. *Biochemistry.* 44:8244–8250.
49. Strauss, H. M., P. Schmieder, and J. Hughes. 2005. Light-dependent dimerisation in the N-terminal sensory module of cyanobacterial phytochrome 1. *FEBS Lett.* 579:3970–3974.
50. Garman, E. F., and G. W. Grime. 2005. Elemental analysis of proteins by microPIXE. *Prog. Biophys. Mol. Biol.* 89:173–205.
51. Sineschekov, V., L. Koppel, B. Esteban, J. Hughes, and T. Lamparter. 2002. Fluorescence investigation of the recombinant cyanobacterial phytochrome (Cph1) and its C-terminally truncated monomeric species (Cph1Delta2): implication for holoprotein assembly, chromophore-apoprotein interaction and photochemistry. *J. Photochem. Photobiol. B.* 67:39–50.
52. Cole, W. J., D. J. Chapman, and H. W. Siegelman. 1967. The structure of phycocyanobilin. *J. Am. Chem. Soc.* 89:3643–3645. [AQ15]
53. Inomata, K., M. A. Hammam, H. Kinoshita, Y. Murata, H. Khawn, S. Noack, N. Michael, and T. Lamparter. 2005. Sterically locked synthetic bilin derivatives and phytochrome Agp1 from *Agrobacterium tumefaciens* form photoinensitive Pr- and Pfr-like adducts. *J. Biol. Chem.* 280:24491–24497.

## QUERIES - biophysj84335q

- [AQ1] Per journal style, all known nonstandard abbreviations have been spelled out at first use in the Abstract and at first use in the main text. Please confirm definitions are correct or edit each instance accordingly.  
Per journal style, spelled-out Greek letters have been replaced with the corresponding symbols throughout the text. Please confirm or edit at each instance.
- [AQ2] Journal style requires that genus and species be written out on first use. “*D. radiodurans*” changed to “*Deinococcus radiodurans*” at first use in Abstract and in main text. Please confirm or amend.
- [AQ3] Please spell out “PPR” at first and only use, per journal style, if appropriate.
- [AQ4] Please provide the location (city and state for USA addresses; city and country for non-USA addresses) of “Isotec”.
- [AQ5] Neither journal style nor the CBE manual allows units of measure with molecular weight, although it does with molecular mass, so “weight” changed to “mass” in both instances. Please confirm or amend.
- [AQ6] Please spell out “DFT” at first use, per journal style, if appropriate.
- [AQ7] Please spell out “GAIO” at first use, if appropriate.
- [AQ8] Please spell out “TDDFT” at first use, if appropriate.
- [AQ9] “EPSRC EPR” spelled out in Acknowledgments, per journal style. Please confirm or amend.
- [AQ10] Per journal style, grant acknowledgements moved to a separate paragraph after general acknowledgments. OK as done?
- [AQ11] Journal title (Phys. Rev.) added to Ref. 38 (Hohenberg and Khon, 1964). Please confirm or amend.
- [AQ12] Reference has only first page number. Please provide the last page number if article is longer than one page. (in reference 44 “Bauernschmitt, Ahlrichs, 1996”). If an Abstract, please so state.
- [AQ13] Reference has only first page number. Please provide the last page number if article is longer than one page. (in reference 45 “Casida, Jamorski, Casida, Salahub, 1998”). If an Abstract, please so state.
- [AQ14] Reference has only first page number. Please provide the last page number if article is longer than one page. (in reference 46 “Adamo, Barone, 1998”). If an Abstract, please so state.
- [AQ15] Cannot find a title to match the journal “J.Am.Chem.Coc.” (in reference 52 “Cole, Chapman, Siegelman, 1967”). Title changed to “J. Am. Chem. Soc.” Please confirm or amend.

# DARTMOUTH JOURNAL SERVICES



Dear Biophysical Journal Author:

We are pleased to inform you that the PDF proof of your article is available for download. If you do not have Adobe Acrobat Reader (software necessary to view the PDF file), please see below.

This PDF is the only set of proofs you will receive for your article. The file should contain one each of the following items:

- ❖ Master proof
- ❖ Query sheet
- ❖ Proofreading marks guide
- ❖ Offprint order form
- ❖ Charge sheet

Please print out the entire file and review your proof carefully. To ensure timely and accurate publication of your article, it is important that you:

- ❖ Answer all queries.
- ❖ Proofread tables and equations for typographical errors.
- ❖ Confirm that Greek and special characters have translated correctly.
- ❖ Mark all changes and corrections in the margin of your proof.
- ❖ Return your proof via overnight express mail, e-mail, or fax within 48 hours of receipt.

NOTE: Returning your proof in a timely manner will secure your place in the issue. Contact us if the return of your proof will be delayed for any reason, or if you would like to be rescheduled for a later issue.

FIGURE RESHOOTS: Please note that your figures will print at a higher resolution than the images in your e-proof. Return high-resolution digital files of any figures that require rework. To avoid the possibility of delay in publication, we also request that you e-mail our office to alert us of incoming reshoots.

DIGITAL PROOFS: If you own the full version of Adobe Acrobat, you may use the highlighting and notes tools to indicate changes directly on the PDF. You may send the corrected proofs as an e-mail attachment to [biophysj@dartmouthjournals.com](mailto:biophysj@dartmouthjournals.com).

Otherwise, kindly return your corrected hard-copy proof and offprint order form to:

Dartmouth Journal Services  
Biophysical Journal  
19 Archertown Road (or Box 275 if USPS)  
Orford, NH 03777

Questions or comments can be sent to: [biophysj@dartmouthjournals.com](mailto:biophysj@dartmouthjournals.com). Thank you for your cooperation; we look forward to processing your article.

Sincerely,

The Editorial Department  
Dartmouth Journal Services

**Special Note:** Adobe Acrobat Reader is available for download free of charge at <http://www.adobe.com/products/acrobat/readstep.html>.

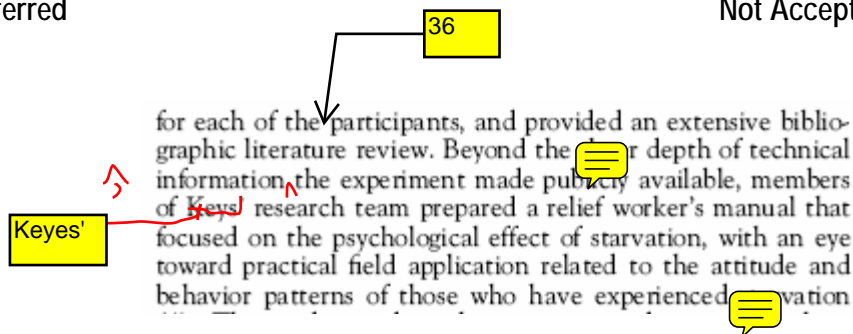
# Proof Correction Guidelines

## Digital Proofs

PDF proofs should be marked up using the standard version of Adobe Acrobat. Please use the Text Box and Pencil tools (v.6: Tools/Advanced Commenting or v.7: Comments/Drawing Markup Tools). Corrections should be made on your proof, not on the query sheet. All corrections should be visible when your PDF file is printed. To ensure accurate and timely processing of your corrections, please do not use the Notes tool. If your corrections are minor, an email or Word document is acceptable.

### Preferred

### Not Acceptable



## Hard Copy Proofs

If you choose to print your eProof and return your corrections via courier, please mark all corrections both in text and in the margin, using standard proofreading marks.

### PROOFREADERS' MARKS

Mark	Meaning and/or example	Mark	Meaning and/or example
	delete <del>take it out</del>		set in <u>roman</u> (roman)
	close up; print as <u>one</u> word		set in <u>boldface</u> (boldface)
	delete and <u>close up</u>		hyphen <u>—</u>
	caret: insert <u>here</u> <u>correction</u>		en dash <1965 <sup>1</sup> / <sub>N</sub> -72>
	insert a <u>space</u> #		em <sup>1</sup> / <sub>M</sub> or long <sup>1</sup> / <sub>M</sub> dash
	slash or shill		superscript (as in CO <sup>2</sup> ) <u>sup</u>
	let marked text stand <u>as set</u> : <u>stet</u>		subscript (as in H <sub>2</sub> O) <u>sub</u>
	transpose <u>change order</u> the		centered ( <sup>1</sup> / <sub>N</sub> for a centered dot in p · t)
	set farther to the left		comma <u>,</u>
	farther to the right		apostrophe <u>'</u>
	indent or insert em quad space		period <u>.</u>
	begin a new paragraph		semicolon <u>;</u>
	set in <u>capitals</u> (CAPITALS)		colon <u>:</u>
	set in <u>small capitals</u> (SMALL CAPITALS)		quotation marks <u>" "</u>
	set in <u>Lowercase</u> (lowercase)		parentheses <u>( )</u>
	set in <u>italic</u> ( <i>italic</i> )		brackets <u>[ ]</u>

# Biophysical Journal 2006

## This is your order form or pro forma invoice

(Please keep a copy of this document for your records)

rev:12/05

This form must be returned to Dartmouth Journal Services with proof, even if no reprints are ordered. All payment information must be completed.

Author Name: \_\_\_\_\_  
Title of Article: \_\_\_\_\_  
Issue of Journal: \_\_\_\_\_  
No. of Pages: \_\_\_\_\_ Manuscript # \_\_\_\_\_

*Please include the journal name and manuscript number or reprint number on your purchase order or other correspondence. Failure to complete purchase order or credit card payment details will result in the article being put on hold.*

### Reprint Costs (Please see charge sheet)

\_\_\_\_\_ number of reprints ordered \$ \_\_\_\_\_  
Color in reprints, \$262.00 per 100 copies \$ \_\_\_\_\_  
Each additional 100, add \$82.00 \$ \_\_\_\_\_  
Each additional ship location, \$32.00 \$ \_\_\_\_\_

**Free color publication does not apply to reprints.**

### Publication Fees (please see charge sheet for details)

#### Regular Articles

##### Page Charges:

##### Members

\$50 per page for pages 1-8 \$ \_\_\_\_\_  
\$100 per page for pages 9-11 \$ \_\_\_\_\_  
\$200 per page for pages 12 and above \$ \_\_\_\_\_

##### Nonmembers

\$70 per page for pages 1-8 \$ \_\_\_\_\_  
\$100 per page for pages 9-11 \$ \_\_\_\_\_  
\$200 per page for pages 12 and above \$ \_\_\_\_\_

Black and white reshoots, \$9.00 each \$ \_\_\_\_\_

Color reshoots, \$60.00 each \$ \_\_\_\_\_

Color Figures, \$400.00 each \$ \_\_\_\_\_

Number of approved free color figures \_\_\_\_\_

#### Biophysical Letters

\$500 flat fee. Fee includes color figure cost, but not author corrections and figure reshoots. Paper must not exceed 3 pages.

**Total Amount Due** \$ \_\_\_\_\_

*Please note that authors of "New and Notable" articles are exempt from publication fees.*

*The author will be notified of additional charges due to excessive corrections to the galley proofs.*

### Invoice Address (Invoice sent after publication)

Name \_\_\_\_\_  
Institution \_\_\_\_\_  
Street \_\_\_\_\_

Department \_\_\_\_\_

City \_\_\_\_\_ State \_\_\_\_\_ Zip \_\_\_\_\_

Country \_\_\_\_\_

Phone \_\_\_\_\_ Fax \_\_\_\_\_

E-mail \_\_\_\_\_

Purchase Order No. \_\_\_\_\_

### Shipping address (Cannot ship to PO Box)

Name \_\_\_\_\_  
Institution \_\_\_\_\_  
Dept. \_\_\_\_\_  
Street \_\_\_\_\_

City \_\_\_\_\_ State \_\_\_\_\_ Zip \_\_\_\_\_

Country \_\_\_\_\_

Quantity \_\_\_\_\_ Fax \_\_\_\_\_

Phone: Day \_\_\_\_\_ Evening \_\_\_\_\_

### Additional Shipping Address\* (Cannot ship to PO Box)

Name \_\_\_\_\_  
Street \_\_\_\_\_

City \_\_\_\_\_ State \_\_\_\_\_ Zip \_\_\_\_\_

Country \_\_\_\_\_

Quantity \_\_\_\_\_ Fax \_\_\_\_\_

Phone: Day \_\_\_\_\_ Evening \_\_\_\_\_

\*Add \$32.00 for each additional shipping address

### Credit Card Payment Details

Credit cards will be processed by DJS and a receipt will be sent with your invoice.

Credit Card: \_\_\_\_\_ VISA \_\_\_\_\_ AMEX \_\_\_\_\_ MasterCard

Card Number: \_\_\_\_\_

Expiration Date: \_\_\_\_\_

Signature: \_\_\_\_\_

Name as it appears on card: \_\_\_\_\_

Billing address of cardholder: \_\_\_\_\_

### Institutional Purchase Order (enclosed)

Send your order form to:  
Dartmouth Journal Services  
Attn. Pat Bertozzi-Buck  
19 Archertown Road  
Box 275  
Orford, NH 03777

Or fax: 603-353-9365

Signature: \_\_\_\_\_

Date: \_\_\_\_\_

Signature is required. By signing this form, the author agrees to accept the responsibility for the payment of reprints and/or all charges described in this document. Failure to pay will impact future publications. Only one invoice per order is provided.

# Biophysical Journal

## 2006 REPRINT AND PUBLICATION CHARGES

### Black and White Reprint Prices

# of pages	Domestic (USA Only)				
	100	200	300	400	500
1-4	\$254	\$273	\$294	\$314	\$334
5-8	\$423	\$459	\$499	\$535	\$576
9-12	\$580	\$637	\$696	\$756	\$814
13-16	\$733	\$813	\$892	\$927	\$1,050
17-20	\$1,047	\$1,165	\$1,290	\$1,407	\$1,525
21-24	\$1,205	\$1,343	\$1,488	\$1,624	\$1,762
25-28	\$1,205	\$1,343	\$1,488	\$1,624	\$1,762
29-32	\$1,363	\$1,518	\$1,688	\$1,843	\$1,999

# of pages	International (includes Canada and Mexico)				
	100	200	300	400	500
1-4	\$275	\$296	\$323	\$350	\$380
5-8	\$447	\$500	\$556	\$609	\$664
9-12	\$612	\$697	\$782	\$865	\$950
13-16	\$777	\$889	\$1,003	\$1,116	\$1,232
17-20	\$947	\$1,087	\$1,233	\$1,373	\$1,514
21-24	\$1,116	\$1,286	\$1,459	\$1,627	\$1,800
25-28	\$1,287	\$1,483	\$1,688	\$1,885	\$2,083
29-32	\$1,438	\$1,680	\$1,919	\$2,139	\$2,367

**Minimum** order is 100 copies. For articles longer than 32 pages, consult the Reprint Department at Dartmouth Journal Services.

### Color in Reprints

Add \$262.00 per 100 copies (and \$82.00 for each additional 100 copies) to the cost of reprints if the article contains any color in addition to black. For color orders greater than 500 copies, please call Dartmouth Journal Services.

### Publication Fees

Please note that "New and Notable" authors are exempt from publication charges. Letter authors pay a \$500 flat fee.

### Corrections

Please note that extensive substantive revisions will need to be approved by the reviewing editor, resulting in the article appearing in a later issue or volume.

Authors will be granted up to an average of two corrections per page at no cost. Corrections, not including printer errors, made to the proofs that exceed two per page will be charged to the author at a rate of \$4.00 per correction. Figures that are replaced through no fault of the journal office or the printer will also be charged to the author.

### Page Charges—Regular Articles

Manuscripts whose corresponding authors are members of the Biophysical Society at the time of original submission pay a reduced \$50 per page fee for pages 1–8, \$100 per page for pages 9–11, and

This order form and prepayment or signed institutional purchase order must be returned to Dartmouth Journal Services within 10 days of receipt.

\$200 per page for pages 12 and over. Page charges for nonmember are \$70 per page for pages 1–8, \$100 per page for pages 9–11, and \$200 per page for pages 12 and above. All authors are expected to pay the page charges for articles they publish in *Biophysical Journal*. Failure to honor page charge obligations will affect future manuscript submissions.

### Page Charges—Biophysical Letters

Authors pay a flat fee of \$500. This includes color figures, but not author corrections and figure reshoots, and paper must not exceed 3 pages.

### Figure Reshoots

If you are submitting figure reshoots, please add \$9.00 for each black and white reshoot and \$60.00 for each color reshoot.

### Articles Published with Color Figures

Color figures that, in the estimation of the Editorial Board with the advice of the referees, are deemed essential to convey the science of the article will be printed free of charge to its authors, provided the corresponding author of the paper is a current member of the Biophysical Society at the time of original submission. In general, color is not necessary for simple line drawings, x-y plots, bar graphs, or simple spectra. For papers submitted by nonmembers, the charge to the authors for all color figures will be \$400 per figure. A Society member may request that color figures be included in one of his or her papers in addition to those approved by the Editorial Board, but the member will be charged for all such color figures at the same rate as nonmembers.

### Shipping

UPS ground within the United States (1–5 days delivery) is included in the reprint prices, except for orders in excess of 1,000 copies. Orders shipped to authors outside the United States are mailed via an expedited air service.

### Multiple Shipments

You may request that your order be shipped to more than one location. Please be aware that it will cost \$32.00 for each additional location.

### Delivery

Your order will be shipped within 2 weeks of the journal print date. Allow extra time for delivery.

### Ordering

Credit card information or a signed institutional purchase order is required to process your order. Failure to complete purchase order or credit card payment details will result in the article being put on hold. Please return your order form, purchase order, and payment to:

Dartmouth Journal Services  
19 Archertown Road  
Box 275  
Orford, NH 03777

Please direct all inquiries to Pat Bertozzi-Buck:

E-mail: pbertozzi@dartmouthjournals.com  
Phone: (603) 353-9360 x105  
Fax: (603) 353-9365